Effect of SiC Addition on Oxidation Behavior of ZrB_2 at 1273 K and 1473 K

Lihua Zhang · Kazuya Kurokawa

Lihua Zhang

Center for Advanced Research of Energy Conversion Materials, Hokkaido University, Kita 13 Nishi 8, Kita-ku, Sapporo 060-8628, Japan

E-mail: zhanglihua@eng.hokudai.ac.jp

Kazuya Kurokawa

Tomakomai National College of Technology, 443 Nishikioka, Tomakomai 059-1275, Japan

E-mail: kurokawa@office.tomakomai-ct.ac.jp

Abstract The oxidation behavior of ZrB_2-SiC composites with different SiC addition was investigated at 1273 K and 1473 K in air for 12 h in this study. The SiC addition contents ranged from 0 to 30wt%. The results showed that when ZrB_2-SiC composites were oxidized at 1273 K in air, a two-oxide layer-structure forms: a continuous glassy layer and a ZrO_2 layer contained unoxidized SiC. When SiC content is 5wt% and 10wt%, the glassy layer is mainly composed by B_2O_3. When SiC content is 20wt% and 30wt%, a borosilicate glass could be formed on the top layer, which could improve the oxidation resistance of ZrB_2. When ZrB_2-SiC composites were oxidized at 1473 K in air, the oxide layer was composed of ZrO_2 and SiO_2 and unreacted SiC. Additionally, when SiC addition content was higher than 10wt%, a continuous borosilicate glass layer could be formed on the top of the oxide layer at 1473 K. With the increase of SiC content in ZrB_2, the oxide layer thickness decreased at both 1273 K and 1473 K.

Keywords Zirconium diboride · Silicon carbide · Oxidation · High temperature

Introduction

Ultra-high temperature ceramics (UHTCs) have been proposed as candidates for applications such as thermal protection systems for hypersonic aerospace vehicles [1,2]. Among the UHTCs, zirconium diboride has the lowest theoretical density (6.09 $g \cdot cm^{-3}$), and has good thermal shock resistance because of its high thermal conductivity (65-135 $W \cdot m^{-1} \cdot K^{-1}$) [3]. These attributes make it attractive for aerospace applications such as thermal protection materials on hypersonic aerospace vehicles and re-usable atmospheric re-entry vehicles. However, the oxidation resistance of ZrB_2 is very poor at temperatures above 1400°C due to the volatilization of B_2O_3, which results in formation of a porous, non-protective ZrO_2 layer. [4,5] Numerous investigations to improve the oxidation resistance of ZrB_2 have been reported. [4,6-11] It was found that SiC addition provided improved oxidation resistance by promoting the formation of borosilicate glass. This borosilicate glass afforded more oxidation protection than B_2O_3 since it is more viscous, has higher melting temperature and lower vapor pressure, and is more protective against oxygen diffusion. [12,13]

The oxidation behaviors of ZrB_2-SiC composites in air have been well-defined previously [6,8-10,14-16]. When ZrB_2-SiC composite is exposed to oxidizing environments, SiC phase begins oxidizing appreciably between 1100°C and 1300°C, resulting in the formation of a silica-rich glassy layer that imparts significant improvement to the oxidation resistance of the diboride at higher temperatures. The SiO_2-containing scale remains protective up to at least 1500°C as SiO_2 is significantly less volatile than B_2O_3 at these temperatures. Thus, ZrB_2-SiC exhibits passive oxidation behavior with parabolic kinetics over a much greater temperature range than has been reported for pure ZrB_2. A. Rezaie *et al.* [17] also reported the oxidation behavior of ZrB_2 with 30 vol% SiC addition at low partial pressure of oxygen. However, the SiC content discussed in these studies is usually in the range of 20 vol% to 30 vol%, and the influence of different SiC addition on the oxidation behavior of ZrB_2 is rarely reported. [18] Therefore, the oxidation of ZrB_2 with different SiC contents is studied in this paper.

Experimental Procedures

Commercially available ZrB_2 and SiC powders were used as raw materials. The ZrB_2-SiC powders with different SiC content (0wt%, 5wt%, 10wt%, 20wt%, and 30wt%) and 1wt% B_4C were measured and then mixed by ball milling. Then, the mixtures were pressureless sintered at 2523 K for 3 h in an Ar atmosphere after metal injection molding process.

The oxidation tests were performed using a horizontal tube furnace. Before the tests, specimens were prepared using conventional polishing with a diamond abrasive, down to a 0.5 μm finish. They were then placed on an alumina boat and inserted into the hot zone of the furnace. The oxidation tests were conducted at 1273 K and 1473 K for 12 h under an air atmosphere.

The densities of the sintered specimens were measured using the Archimedes method, and the theoretical densities of the composites were calculated using the rule of mixture. The microstructures of the cross-sections of the oxidized specimens were characterized using scanning electron microscopy (SEM). To analyze the microstructures of the vertical sections after the tests, the specimens were cross-sectioned and mounted in epoxy, carefully polished with a diamond abrasive down to a 0.5 μm finish, and cleaned in an ultrasonic bath. The thicknesses and element profiles of the resulting reaction layers were measured and analyzed from the polished cross-sections by energy dispersive spectrometer (EDS).

Results and Discussion

(1) Density and microstructure

Table 1 shows the density of the specimens obtained. The relative densities of the specimens before oxidation test is in the range of 96%-99%.

Fig. 1 shows SEM images of the polished surfaces of the ZrB_2-SiC composites. The darker phase is SiC, and it appears to be uniformly dispersed in the lighter ZrB_2 matrix. The microstructures of composites are regular, and little pore was observed in the polished surfaces. Based on the high relative density and the lack of any open pores, porosity should not have a significant effect on oxidation behavior.

(2) Oxidation behavior at 1273 K

Thermodynamically, both ZrB_2 and SiC should be oxidized when exposed to air. However, the oxidation rates of both species are negligible below about 1073 K [19]. Previous studies have reported that the oxidation of ZrB_2 by Reaction (1) is much faster than that of SiC between 1073 and 1473 K [20,21]. Assuming that oxidation of ZrB_2 proceeds stoichiometrically, the reaction should produce molten B_2O_3 (melting temperature ~723 K) and solid ZrO_2. Upon cooling to room temperature, the B_2O_3 forms an amorphous solid while the ZrO_2 is crystalline [18].

$$ZrB_2(s) + \frac{5}{2}O_2(g) = ZrO_2(s) + B_2O_3(l) \quad (1)$$

Fig. 2 shows the SEM images of ZrB_2-SiC specimens with different SiC addition contents after exposure to air for 12 h at 1273 K. As shown in the figure, the surface of oxide layer is fragile and easy to have crack and spallation, and it is easy to be exfoliated during cutting and polishing process. In order to observe the oxide layer clearly, the cross-section of ZrB_2-SiC specimens without polishing are analyzed by EDS. Fig. 3 shows the EDS maps for ZrB_2-10%SiC specimens after oxidation at 1276 K in air for 12 hours. The inserted table shows the mole ratio of the elements C, O, Si and Zr of red mark point in Fig. 3(a). As the K_α of boron is 0.183, which is lower than the detection limit of the equipment used, the boron element is very difficult to be detected. According to the mole ratio of O and Si, it could be found out that the glassy layer is mainly composed by B_2O_3. A. Rezaie *et al.* [19] reported that the surface structure consisted of 3 layers after the oxidation of ZrB_2-SiC at 1273 K for 30 min: (1) a layer of B_2O_3, (2) a ZrO_2 layer

contained unoxidized SiC, (3) unaffected ZrB_2-SiC. Therefore, a continuous B_2O_3 layer formed above the ZrO_2 layer was found in the reported study. As shown in Fig. 3, a glassy layer of B_2O_3 is on the top of the surface. The maps of Zr, Si, C and O show that a ZrO_2 layer with SiC is under B_2O_3 layer, and the thickness of this layer is larger than that of B_2O_3 layer. Therefore, the two-layer-structure was found in the oxide layer of ZrB_2-10%SiC specimen.

Fig. 4 shows EDS maps of ZrB_2-20%SiC specimen after oxidation at 1273 K and the inserted tables show the point analysis of the red mark points. Different with the ZrB_2-10%SiC specimen, the carbon element was not detected on the top oxide layer, which means that SiO_2 exists in the top layer. Additionally, the relatively higher ratio of O indicate the composition of B_2O_3 should also exist in the top layer. This means that a borosilicate glass is formed on the top layer. The maps of Zr, Si, O and C show that ZrO_2 with SiC is under the glassy layer, which is same as that of the ZrB_2-10%SiC specimen. Therefore, when SiC content increased, some SiO_2 is formed and the formation of SiO_2 could be accelerated by the presence of B_2O_3 [22].

Fig. 5 shows the thickness of the oxidation layer of ZrB_2-SiC composites. With the increase of SiC addition content, the oxide layer thickness decreased. It was reported that SiC additions do not affect the oxidation rate below 1373 K. However, in this work the increase of SiC addition shows an increase oxidation resistance of ZrB_2 at 1273 K. Y. H. Seong *et al.* [23] reported that the oxidation kinetics of ZrB_2 might be controlled by O_2 diffusion and transport through the ZrB_2 grain boundaries and ZrO_2 grain boundaries, respectively. Although the oxidation of SiC is much slower than that of ZrB_2 at 1273 K, when SiC content is higher than 10wt% in our experimental conditions, SiO_2 forms in the top glassy layer, which could decrease the diffusion of oxygen.

3.3 Oxidation behavior at 1473 K

When ZrB_2-SiC was heated at 1473 K, the composition and structure of the surface layers changed. As the temperature approaches 1473 K, the vapor pressure of B_2O_3 increases, leading to its rapid evaporation. In addition, SiC starts to oxidize to produce SiO_2 and CO. According to K. Shugart *et al.*[24] study, B_2O_3 does not completely evaporate even at 1773 K, thus little B_2O_3 should be still remained in the oxide layer. Fig. 6 shows the SEM images of ZrB_2-SiC specimens with different SiC addition contents after exposure to air for 12 h at 1473 K. An apparent oxide layer is formed for ZrB_2-SiC compositions. Fig. 6 (d) shows that the

oxide layer is not as compact as the unaffected ZrB_2-SiC and some pores are visible in the oxide layer. When SiC addition content is 5wt%, a two-layer-structure is formed as follows: (1) a layer of ZrO_2 and SiO_2 with unreacted SiC; (2) unaffected ZrB_2-SiC. As a little boron is detected in oxide layer, it is considered that a small amount of B_2O_3 is still remain in the oxide layer. However, when SiC addition content is higher than 10wt%, a continuous molten layer could be observed. As the melting point of SiO_2 is higher than 1700 K, a borosilicate glass layer is formed on the top of the oxide layer.

According to the reported TEM study of the oxide layer on ZrB_2-SiC [23], ZrB_2 was oxidized and transformed to ZrO_2 phase firstly and then SiC was oxidized at the interface between unreacted layer and oxidized layer during the oxidation. Fig.7 (b) shows that SiC started to oxidize and transform into SiO_2 from the surface of SiC grain. After that, the SiO_2 was dispersed in grain boundaries in whole oxide layer on composite due to high viscosity and volumetric increase. The unreacted SiC existed in amorphous SiO_2.

Fig. 8 shows the thickness of the oxidation layer of ZrB_2-SiC composites. The addition of SiC greatly decreases the oxide layer thickness because of the SiO_2 formation. When SiC content is 5wt%, the oxide layer thickness is almost half of that without SiC addition. When the SiC content increased from 5% to 30wt%, the oxide layer thickness decreased gently. This result proved that increase of SiC addition could effectively improve the oxidation resistance of ZrB_2. In all the specimens, ZrB_2 containing 30 wt% SiC exhibited the highest oxidation resistance at 1473 K in air.

Conclusions

The oxidation behavior of ZrB_2-SiC composites with different SiC contents was investigated at 1273 K and 1473 K in air for 12 h. The following conclusions could be obtained:

(1) When ZrB_2-SiC composite is oxidized at 1273 K in air, a two-oxide layer-structure forms: a continuous glassy layer and a ZrO_2 layer contained unoxidized SiC. When SiC content is 5wt% and 10wt%, the glassy layer is mainly composed by B_2O_3. When SiC content is 20wt% and 30wt%, a borosilicate glass could be formed on the top layer, which could improve the oxidation resistance of ZrB_2.

(2) When ZrB_2-SiC composite is oxidized at 1473 K in air, the oxide layer is composed of ZrO_2 and SiO_2 with unreacted SiC. When SiC addition content is higher than 10wt%, a continuous borosilicate glass layer could be formed on the top of the oxide layer.

(3) With the increase of SiC content in ZrB_2, the thickness of oxide layer decreased at both 1273 K and 1473 K. The addition of SiC shows effective protection of ZrB_2 at 1473 K.

(4) In all the specimens, ZrB_2 containing 30 wt% SiC exhibits the highest oxidation resistance at 1473 K in air.

References

1) M. M. Opeka, I. G. Talmy, J. A. Zaykoski, *Journal of Materials Science*, 39, 5887-5904 (2004).
2) F. Monteverde, A. Bellosi, S. Guicciardi, *Journal of the European Ceramic Society*, 22, 278-288 (2002).
3) R. A. Cutler, *Engineeried Materials Handbook Volume 4: Ceramics and Glasses* (Engineering Properties of Borides, S. J. Schneider, 1991)
4) W. C. Tripp, H. C. Graham, *Journal of the Electrochemical Society*, 118, 1195-1209 (1971).
5) W. G. Fahrenholtz, *Journal of the American Ceramic Society*, 88, 3509-3512 (2005).
6) S. R. Levine, E. J. Opila, M. C. Halbig, J. D. Kiser, M. Singh, J. A. Salem, *Journal of the European Ceramic Society*, 22, 2757-2767 (2002).
7) A. K. Kuriakose, J. L. Margrave, *Journal of the Electrochemical Society*, 111, 827-831 (1964).
8) E. J. Opila, M. C. Halbig, *Ceramic Engineering & Science Proceedings*, 22, 221-228 (2001).
9) A. L. Chamberlain, W. G. Fahrenholtz, G. E. Hilmas, *Refractories Applications Transactions*, 1 (2005), 1-8.
10) F. Monteverde, A. Bellosi, *Journal of the Electrochemical Society*, 150, B552-B569 (2003).
11) D. Sciti, M. Brach, A. Bellosi, *Journal of Materials Research*, 20, 922-930 (2005).
12) W. G. Fahrenholtz, G. E. Hilmas, I. G. Talmy, J. A. Zaykoski, *Journal of the American Ceramic Society*, 90, 1347-1364 (2007).
13) S. S. Hwang, A. L. Vasiliev, N. P. Padture, *Materials Science and Engineering: A*, 464, 216-224 (2007).
14) P. Hu, W. Guolin, Z. Wang, *Corrosion Science*, 51, 2724-2732 (2009).
15) W. G. Fahrenholtz, *Journal of the American Ceramic Society*, 90, 143-148 (2007).
16) A. Rezaie, W. G. Fahrenholtz, G. E. Hilmas, *Journal of the American Ceramic Society*, 89, 3240-3245 (2006).
17) P. A. Williams, R. Sakidja, J. H. Perepezko, P. Ritt, *Journal of the European Ceramic Society*, 32, 3875-3883 (2012)
18) W. Han, P. Hu, X. Zhang, J. Hang, S. Meng, *Journal of the American Ceramic Society*, 91, 3328-3334 (2008).
19) A. Rezaie, W. G. Fahrenholtz, G. E. Hilmas, *Journal of the European Ceramic Society*, 27, 2495-2501 (2007).
20) W. C. Tripp, H. H. Davis, H. C. Graham, *Am. Ceram. Soc. Bull.*, 52, 612-613 (1973).

21) W. C. Tripp, H. C. Graham, *Journal of the Electrochemical Society*, 118, 1195-1199 (1968).

22) C. E. Ramberg, G. Cruciani, K. E. Spear, R. E. Tressler, C. F. Ramberg. *Journal of the American Ceramic Society*, 79, 2897-2911 (1996).

23) Y. H. Seong, S. J. Lee, D. K. Kim, *Journal of the American Ceramic Society*, 96, 1570-1576 (2013).

24) K. Shugart, S. Liu, F. Craven, E. Opila, *Journal of the American Ceramic Society*, 98, 287-295 (2015).

Table 1 Summary of ZrB_2-SiC specimens: compositions, designations, bulk densities, theoretical densities, and relative densities

Samples	Compositions			Bulk densities ($g \cdot cm^{-3}$)	Theoretical densities ($g \cdot cm^{-3}$)	Relative densities (%)
	ZrB_2 (wt%)	SiC (wt%)	B_4C (wt%)			
ZrB_2	99	0	1	5.79	6.00	96.5
ZrB_2-5%SiC	94	5	1	5.59	5.75	97.2
ZrB_2-10%SiC	89	10	1	5.37	5.52	97.3
ZrB_2-20%SiC	79	20	1	5.01	5.10	98.2
ZrB_2-30%SiC	69	30	1	4.65	4.75	97.9

Captions

Fig. 1 Cross-sectional images of (a) ZrB_2-5%SiC, (b) ZrB_2-10%SiC, and (c) ZrB_2-30%SiC

Fig. 2 SEM images of cross section of ZrB_2-SiC specimens after exposure to air for 12 h at 1273 K. (a) without SiC addition; (b) ZrB_2-5%SiC; (c) ZrB_2-10%SiC; (d) ZrB_2-20%SiC; (e) ZrB_2-30%SiC.

Fig. 3 EDS maps for ZrB_2-10%SiC specimen after oxidation at 1273 K in air for 12 h. (a) SEM images of the cross section; (b) Zr map; (c) Si map; (d) C map; (e) O map. The inserted table is the analysis of the red point in (a).

Fig. 4 EDS maps for ZrB_2-20%SiC specimen after oxidation at 1273 K in air for 12 h. (a) SEM images of the cross section; (b) Zr map; (c) Si map; (d) O map; (e) C map. The inserted tables are the analyses of the red points in (a).

Fig. 5 Thickness of oxide layer of ZrB_2-SiC composites after exposure to air for 12 h at 1273 K.

Fig. 6 SEM images of cross section of ZrB_2-SiC specimens after exposure to air for 12 h at 1473 K. (a) ZrB_2-5%SiC; (b) ZrB_2-10%SiC; (c) ZrB_2-20%SiC; (d) ZrB_2-30%SiC.

Fig. 7 SEM images of cross section of ZrB_2-SiC specimens after exposure to air for 12 h at 1473 K. (a) ZrB_2-30%SiC; (b) high magnification of square area of (a).

Fig. 8 Thickness of oxide layer of ZrB_2-SiC composites after exposure to air for 12 h at 1473 K.

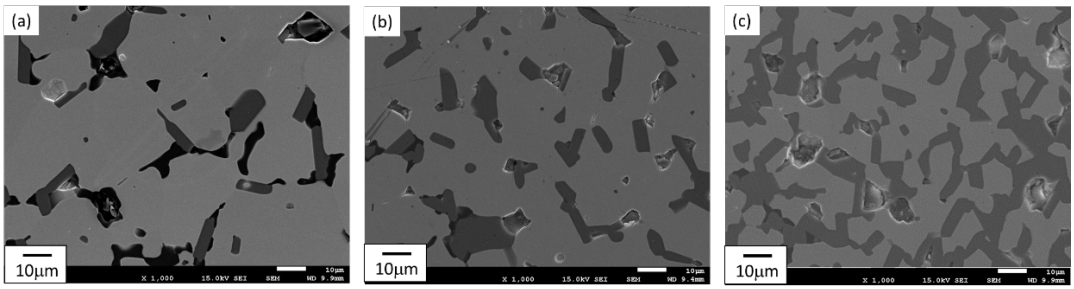

Fig. 1 Cross-sectional images of (a) ZrB_2-5%SiC, (b) ZrB_2-10%SiC, and (c) ZrB_2-30%SiC

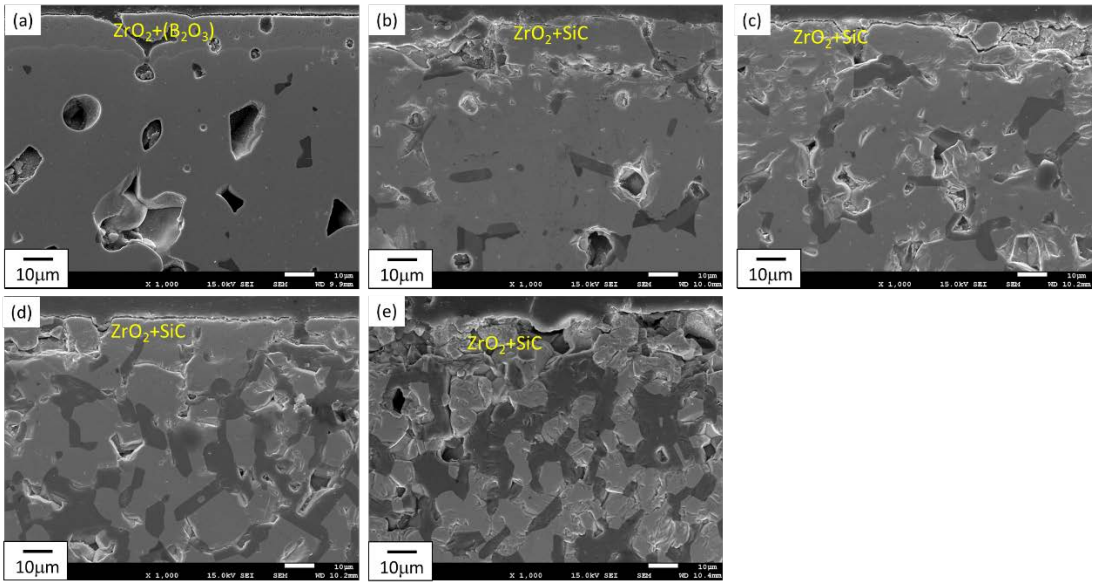

Fig. 2 SEM images of cross section of ZrB_2-SiC specimens after exposure to air for 12 h at 1273 K. (a) without SiC addition; (b) ZrB_2-5%SiC; (c) ZrB_2-10%SiC; (d) ZrB_2-20%SiC; (e) ZrB_2-30%SiC.

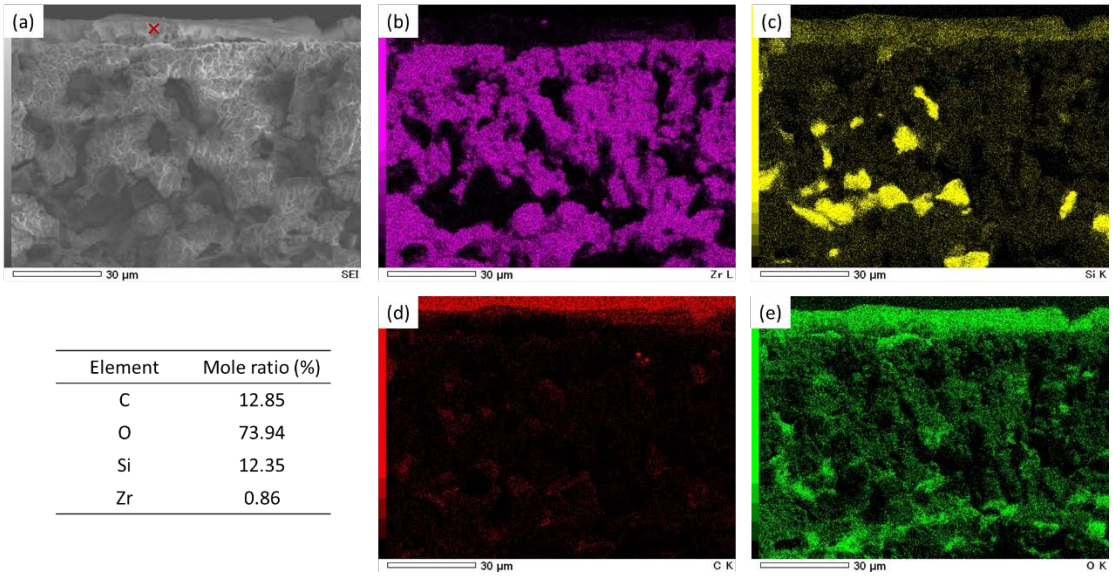

Element	Mole ratio (%)
C	12.85
O	73.94
Si	12.35
Zr	0.86

Fig. 3 EDS maps for ZrB_2-10%SiC specimen after oxidation at 1273 K in air for 12 h. (a) SEM images of the cross section; (b) Zr map; (c) Si map; (d) C map; (e) O map. The inserted table is the analysis of the red point in (a).

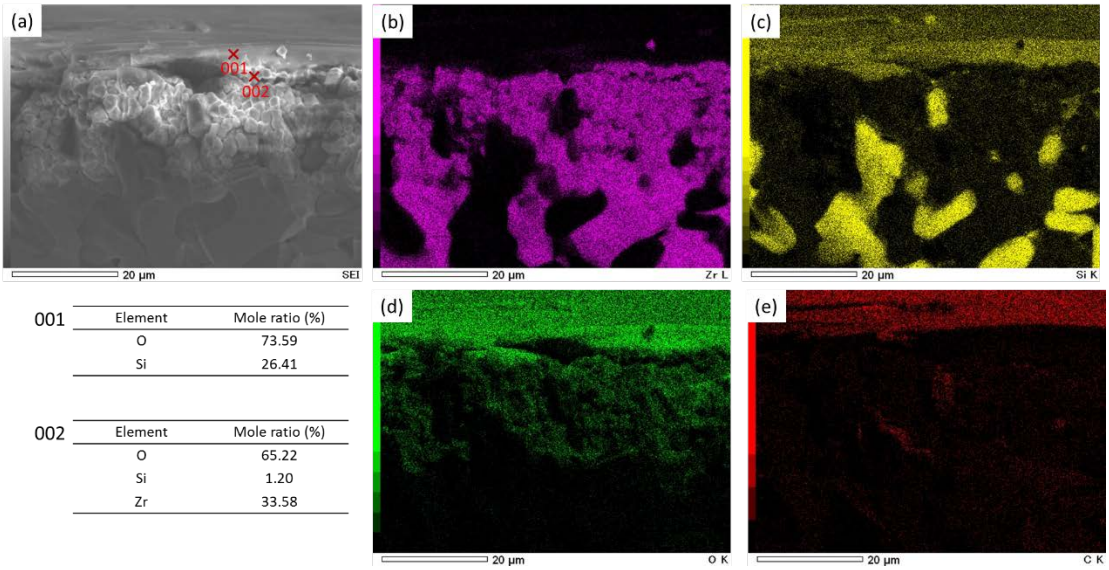

001

Element	Mole ratio (%)
O	73.59
Si	26.41

002

Element	Mole ratio (%)
O	65.22
Si	1.20
Zr	33.58

Fig. 4 EDS maps for ZrB_2-20%SiC specimen after oxidation at 1273 K in air for 12 h. (a) SEM images of the cross section; (b) Zr map; (c) Si map; (d) O map; (e) C map. The inserted tables are the analyses of the red points in (a).

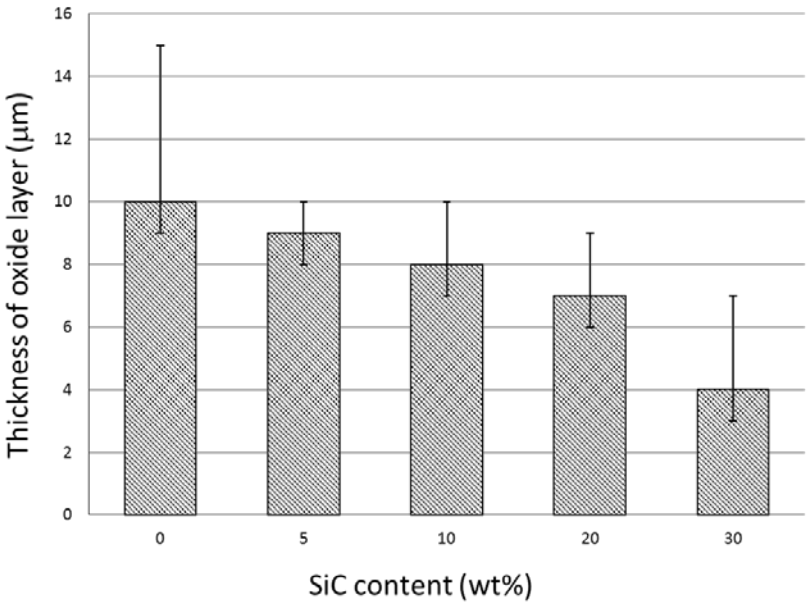

Fig. 5 Thickness of oxide layer of ZrB_2-SiC composites after exposure to air for 12 h at 1273 K.

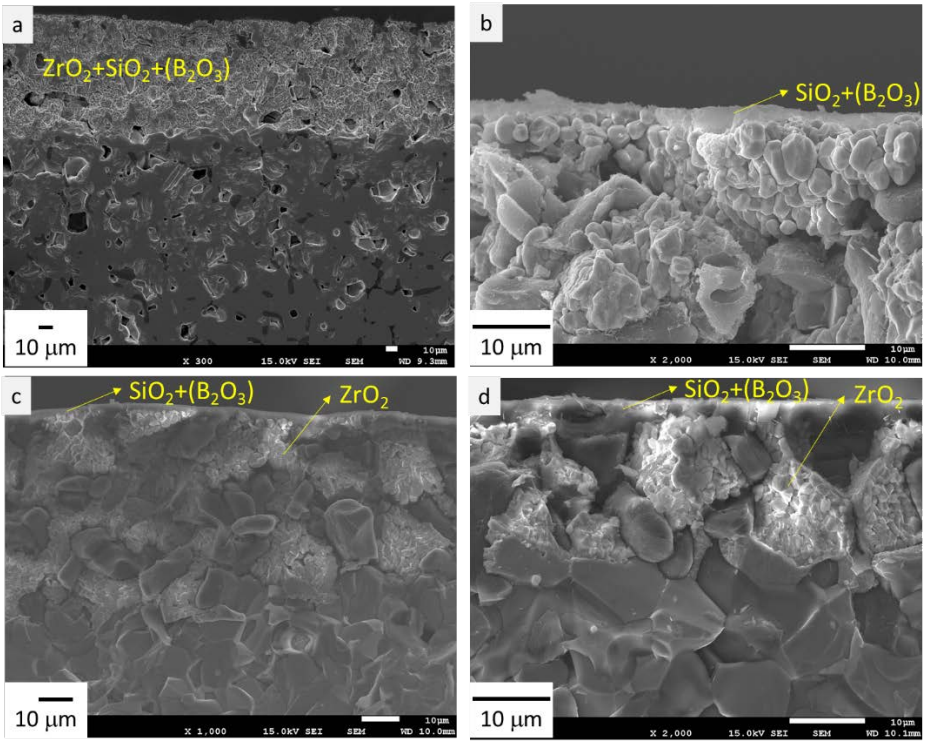

Fig. 6 SEM images of cross section of ZrB_2-SiC specimens after exposure to air for 12 h at 1473 K. (a) ZrB_2-5%SiC; (b) ZrB_2-10%SiC; (c) ZrB_2-20%SiC; (d) ZrB_2-30%SiC.

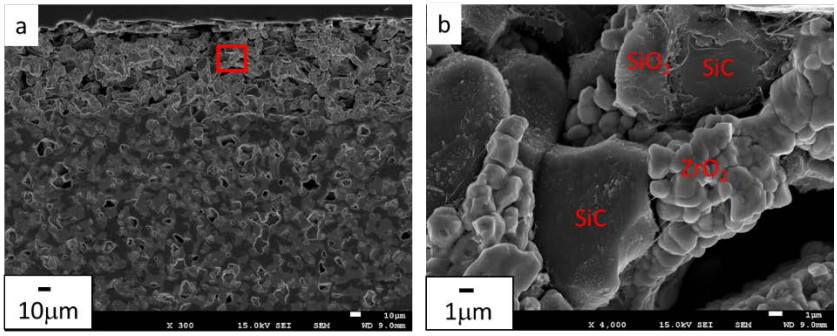

Fig. 7 SEM images of cross section of ZrB_2-SiC specimens after exposure to air for 12 h at 1473 K. (a) ZrB_2-30%SiC; (b) high magnification of square area of (a).

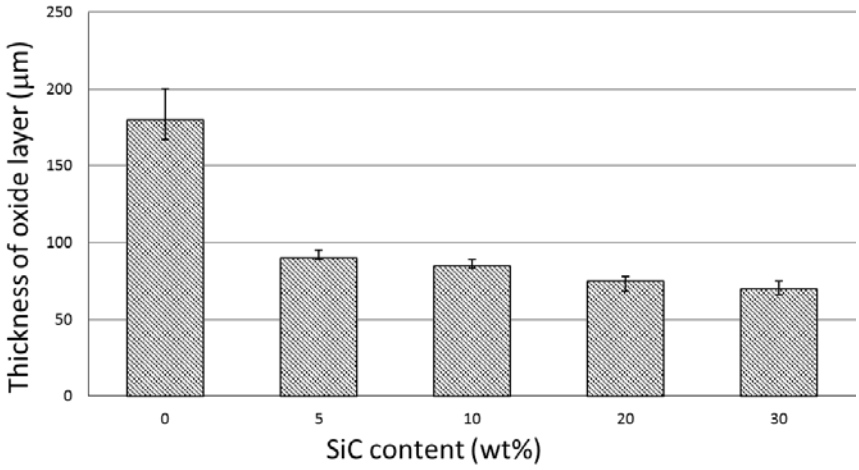

Fig. 8 Thickness of oxide layer of ZrB_2-SiC composites after exposure to air for 12 h at 1473 K.